Preliminary Design Study on Non-Twisted HTS Conductor for Fusion Applications

S. Oh , H. W. Kim , S. Nam , Y. Chu, D. K. Oh , H. Choi, J. T. Lee , W. Kim , Y. S. Jeong, H. Chang, J. Lee , and S. Hahn

Abstract—**Full transposition of superconducting wires within a conductor may not be a requirement for high temperature superconductor (HTS) magnet for fusion applications. Already, conduction-cooled 20 T model coil built with non-transposed HTS stacks has been demonstrated by Commonwealth Fusion Systems (CFS). Here, we discuss 3 possible stacked HTS cryogen-cooled conductor concepts for toroidal field (TF) magnet applications. The first one is somewhat like LTS conductors, the second, HTS stacks are capped by copper stabilizer, the last one, only stacks without copper. We simulate a simplified TF magnet model, 12 T, size of KSTAR, using the 3 conceptual HTS conductor designs. A comparative thermo-hydraulic analysis for a fast charging case has been carried out and its implications on HTS conductor design are further discussed.**

Index Terms—**Fusion magnet, hysteresis loss, high temperature superconductor, stacks-in-conduit conductor.**

I. INTRODUCTION

MORE than 30 years research of conductors for fusion leads us to solidify lots of design issues [1]. One of the early consensus is superconducting cables, constituting cable-in-conduit conductors (CICC), need to be fully transposed. If not, due to inductance mismatch, uneven current distribution occurs, lowering its performance. Also, full transposition is quite effective in reducing coupling loss. On the other hand, for HTS cables, it was recently reported that simply stacked, non-transposed HTS cables' inductance variation is typically less than 2%, capable of more or less uniform current flow [2]. The reduction of AC loss by twisting typically less than 36% for HTS cables [2]. If we do not need to transpose, then fabrication process will become much easier.

For a low temperature superconductor (LTS) conductor, cabling schemes, the amount of copper stabilizer, void fraction and so on can be regarded as important early stage design parameters. As an example, the amount of copper is conservatively decided based on Stekly criterion and hot spot temperature [3]. In case of HTS conductors, however, design parameters does not seem to be settled down yet. For a simply stacked HTS, non-localized heat generation due to hysteresis loss alone is way beyond high as compared with local disturbance considered for the design of LTS conductors [4]. As a result, the 20 T model coil recently demonstrated by CFS [5] only can be charged very slowly, as the coil as a whole and its constituent non-transposed HTS tapes are conduction cooled.

In this work, we consider 3 stacked HTS conductor design concepts cooled by cryogen and will present comparative analysis results. The first concept, similar to LTS conductors, has a bit porous cryogen flow path, the second one has separated copper and HTS segments and final one does not have any stabilizer. About KSTAR size toroidal field (TF) magnet with maximum field of 12 T is assumed as a design base line. If hysteresis loss is the major source of external disturbance then charging and discharging process can be argued as the most vulnerable situation. A thermo-hydraulic analysis for a charging case has been carried out by using SUPERMAGNET code, a part of the Cryosoft package.

II. 3 CONCEPTUAL DESIGNS AND ANALYSIS SCHEME

A. Design Basis and 3 Conceptual Designs

The biggest merit of using HTS for fusion applications is its ability to generate higher magnetic field as compared with LTS. As noted, 20 T TF model coil has been already demonstrated [5]. However, here we instead study a lower field case, 12 T field and size of the KSTAR magnet [6]. Configuration study inside a conduit is our main focus. An easier case can be a better starting point. It is assumed TF magnet is made of HTS conductors which has the same size of conduit, the same winding pack, 8 turns and 7 layers double-pancake windings as those of KSTAR [7]. From a scaling approach, we can expect if we increase TF current from 35.2 kA, the operation current of KSTAR, to 56.7 kA than the peak field will increase from 7.5 T to 12 T. Any complexity arising with the increase of Lorentz force is not considered here.

Fig. 1. (a) Planar array module. (b) Simply stacked module.

Fig. 2. Cross-sectional view of 3 conceptual designs. In the inset of (a), 3D view of SICC I is presented as well. In (b) and (c), alternative designs are shown together. For SICC II, major cryogen flow can be bounded on the copper block. For SICC III, additional supporting structure can be added, if needed.

Fig. 3. (Left) cryogenic circuit model. Circulator is represented as triangle in the bottom. (Right) winding pack scheme and representative DP studied in this work as a part of the circuit model.
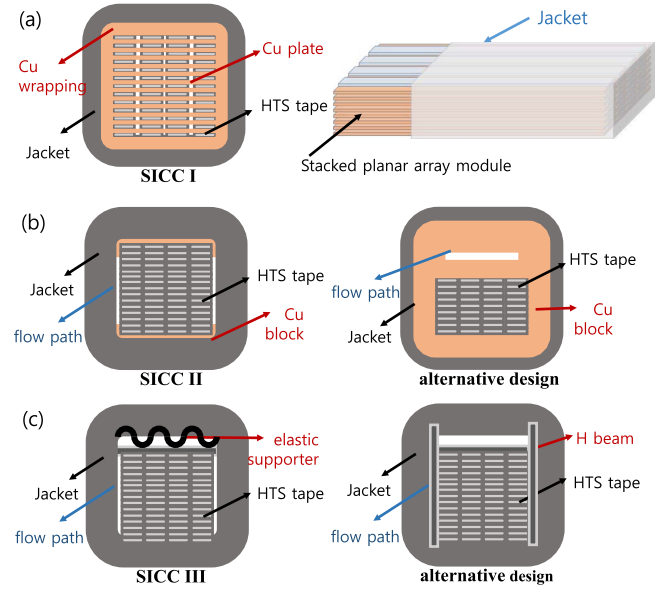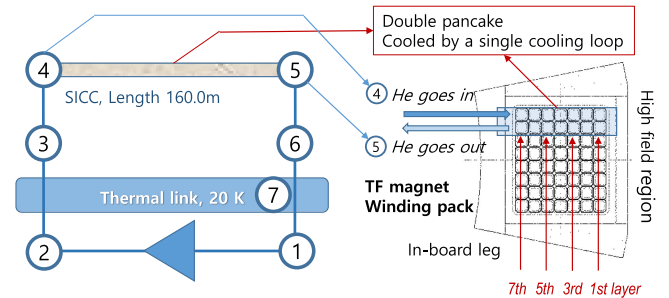
We set the operation temperature to 20 K. It was recently reported cooling power at 20 K by forced flow helium is comparable or even better than any other cryogen, such as neon or hydrogen [8]. The current sharing temperature is above 40 K. Enough margin for a safe operation is also considered as an important design constraint. If we were to use commonly available HTS tapes about 4 mm wide and 0.1 mm thick, for example, manufactured by Superpower or Sunam, then we found about 600 HTS tapes are needed for each conductor to meet the above constraints. The critical current of considered tapes at 12 T, 40 K is above 99 A.

Stacking 600 tapes into a conduit all at once may be possible but will be very tricky. We propose two stacking module concepts as schematically shown in Fig. 1. The first one uses thin copper or copper-coated SUS tapes, on which several HTS tapes are partially or fully soldered in parallel. The other one stacks 30 to 40 tapes and then wrapped by copper or SUS. If we were to use 30 tapes stacked modules than on the final assembly tray, only 20 modules will be arranged, simplifying the procedure. The other merit of using these modules is that tapes can be appended by partial soldering as depicted in Fig. 1 so that the length of modules can be prolonged even though there is a limitation in the length of HTS tapes.

Using the above modules, 3 conceptual designs are proposed as presented in Fig. 2. The first one, using the first module, a thin copper layer and an array of HTS tapes are alternately stacked. Overall stacks are wrapped before put into a conduit. Cryogen flows along the narrow spaces in between parallelly arrayed HTS tapes, similar to LTS conductors where cryogen flows through voids in cables. The second and the third use the second module. The second concept is similar to that of already reported HTS conductors [9], [10], [11], where HTS stacked tapes whether twisted or not are secured by copper blocks and cryogen mainly flows through holes in the copper blocks. The third one is a bit aggressive, no copper stabilizer is used. We will call these HTS conductors as stacks-in-conduit conductors (SICC) similar to CICC for LTS conductors. The first concept will be referred as SICC I, the second as SICC II, and the third, SICC III.

B. Thermo-Hydraulic Analysis Scheme

If the heat load due to AC loss is pretty high, then how cryogen can remove that heat load also can be regarded as critical. A simple cryogenic circuit as shown in Fig. 3, in the left side, is used for a thermo-hydraulic analysis. 10 bar pressurized helium is supplied by a circulator, which is assumed to follow parabolic equation, $\dot{m} = \dot{m}_0 \left(1 - ((p_\text{in} - p_\text{out})/\Delta p_0)^2\right)$, where $\dot{m}$, $\dot{m}_0$, p_in, p_out and Δp_0 are mass flow rate, the maximum flow rate, circulator inlet and outlet pressure, and the pressure head, respectively. There may be optimized circulator settings for each specific conductor configuration, but here we set $\dot{m}_0$ and Δp_0 to 24 g/sec and 2.5 bar, similar to KSTAR operation conditions [12]. The number in the circle corresponds to volume node number of FLOWER input file. Our SUPERMAGNET model consists of one FLOWER and one THEA model. Most of the circuit are simulated by FLOWER model but the SICC in-between nodes 4 and 5 are described by THEA model.

As shown in the right side of Fig. 3, the SICC described by the THEA model corresponds to only one double pancake (DP) out of 4, constituting the winding pack. The cooling lines goes in parallel for each DP, therefore this simplified circuit can be a good representative for the whole TF magnet. As a further simplification, it is assumed that the magnetic field of SICC
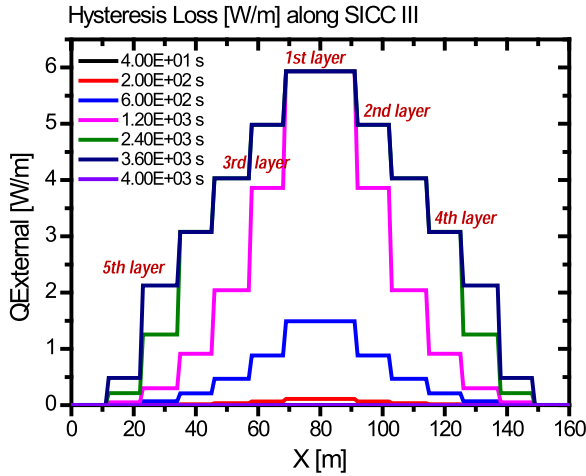
Fig. 4. Hysteresis loss profile variations during the magnet charging process. A fast ramping, 50 kA/hour case is considered and the same heat is applier for the other SICCs, as well.

TABLE I
THEA INPUT FILE KEY PARAMETERS

Parameter	SICC I	SICC II	SICC III
Thermal Parameters			
(HTS) Hatelloy area	$2.38{\times}10^{-4}$ m^2	$2.38{\times}10^{-4}$ m^2	$2.38{\times}10^{-4}$ m^2
(HTS) ReBCO area	$4.86{\times}10^{-6}$ m^2	$4.86{\times}10^{-6}$ m^2	$4.86{\times}10^{-6}$ m^2
Copper stabilizer area	$9.03{\times}10^{-5}$ m^2	$4.91{\times}10^{-5}$ m^2	-
SUS supporter area*	-	-	$1.6{\times}10^{-5}$ m^2
Hydraulic Parameters			
Cryogen flow area	$5.78{\times}10^{-5}$ m^2	$5.78{\times}10^{-5}$ m^2	$9.09{\times}10^{-5}$ m^2
Hydraulic diameter	$1.77{\times}10^{-4}$ m	$3.02{\times}10^{-3}$ m	$2.82{\times}10^{-3}$ m
Wetted perimeter**	$1.22{\times}10^{-1}$ m	$3.05{\times}10^{-2}$ m	$3.05{\times}10^{-2}$ m

*Only the area of capping SUS is consider not that of elastic supporter.
**Wetted perimeter of HTS stack.

located on the same layer is the same. In other word, the magnetic field along the SICC increases stepwisely, reaches its maximum in the middle then decreases stepwisely, and so does hysteresis loss as shown in Fig. 4. Hysteresis loss is approximated by an infinite slab model [13], [14],

$$Q = \frac{2}{3\mu_0} \frac{B^3}{B_p}, \, B < B_p$$

$$Q = \frac{2B_p}{\mu_0}\left(B - \frac{2}{3}B_p\right), \, B < B_p$$

The penetration field is given by $B_p = \mu_0 \, J_{sc} d/2$, where J_{sc} is the critical current density and d is the thickness of HTS stack.

Some THEA input file parameters are listed in Table I. Superconductor parameters were adopted from Superpower HTS tape material properties, which were also used for the quench analysis of CROCO conductors [15]. The heat transfer in-between cryogen and solid was modeled by using Dittus-Boelter (DB) correlation as it was for the CROCO analysis and for the cryogen flow friction, by Blasius equation. HTS tape is assumed to consist of Hastelloy substrate and ReBCO layer only. Copper will be definitely needed at least to facilitate current transfer among
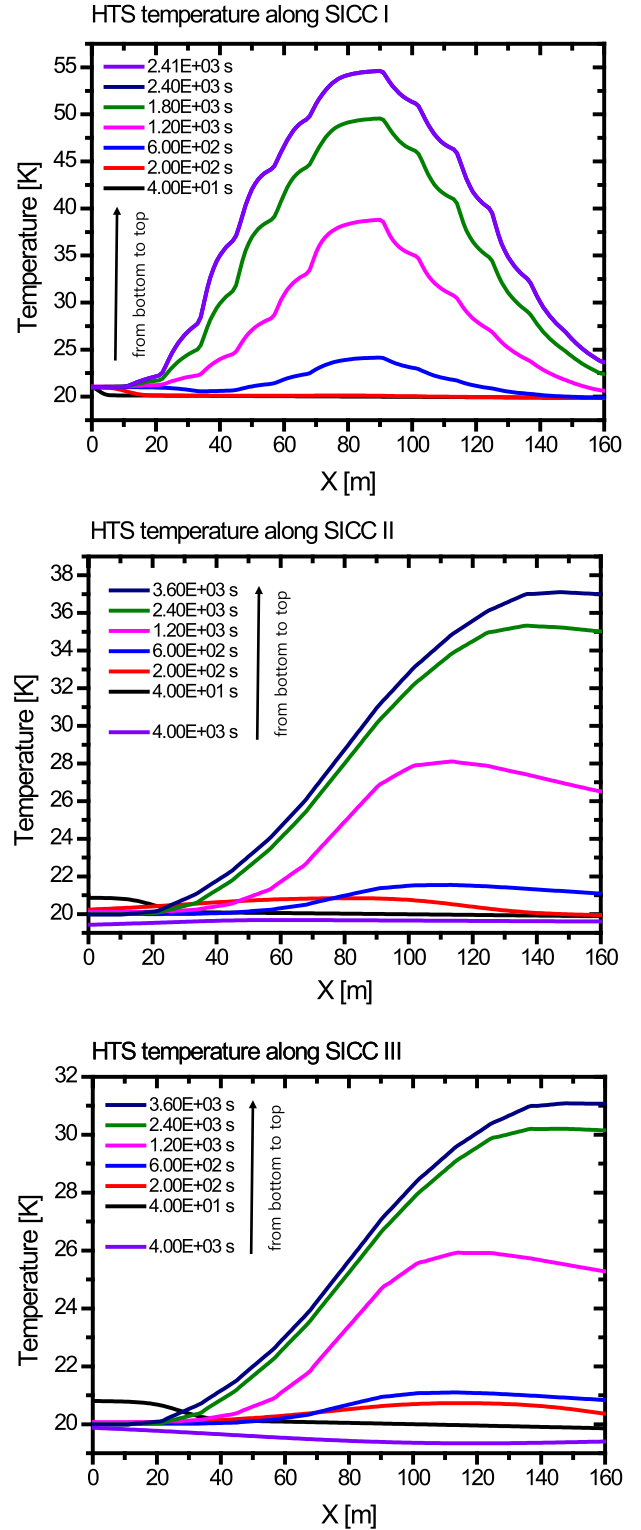

Fig. 5. Temperature profile variations during the magnet charging process.

HTS tapes. But here, we are mainly interested in its impact on thermo-hydraulic characteristics by its thermal conductivity or heat capacity, we studied a sort of ideal case without copper. So that for the SICC III case, there is no copper inside the conduit.
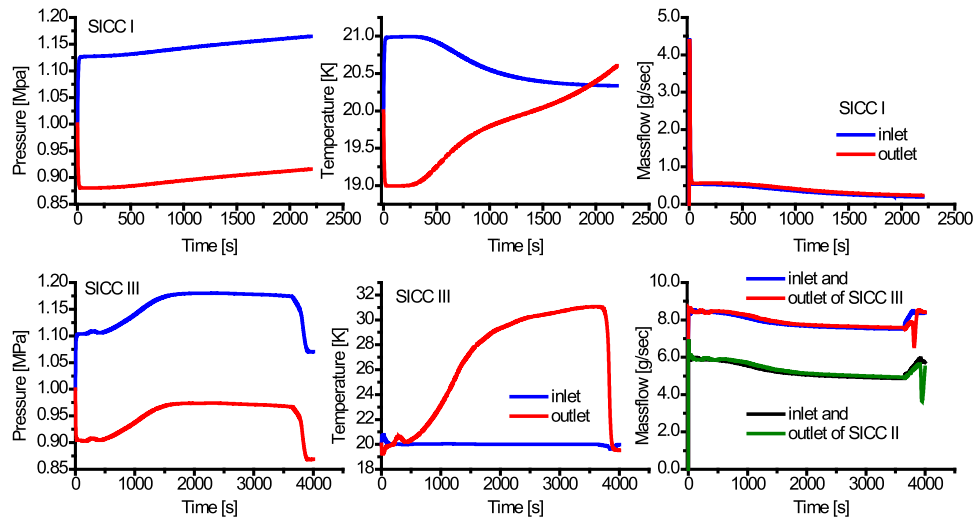
Fig. 6.   Pressure, temperature and mass flow variations at the inlet and outlet (near the volume node 4 and 5, respectively, shown in left side of Fig. 3) for SICC I (top) and SICC III (bottom). The mass flow rate for SICC II is also presented together (bottom right).

Cryogen flow area is about 1.6 times larger for the SICC III case as compared with those of others, whereas the hydraulic diameter of SICC I is an order of magnitude smaller.

III. RESULTS AND DISCUSSION

For TF magnet applications, it is not necessary to charge the magnet fast. But in this work, a high current ramping, 50 kA/hour case, the ramp rate of $\sim$2.9 mT/sec, is considered. At this ramping rate, the hysteresis loss grows as high as $\sim$6 W/m, as presented in Fig. 4. Aside hysteresis loss, there can be a variety of heat loads in an actual fusion device, but most of them localized, spatially or temporally. How the huge non-local, an hour-long hysteresis loss are removed depending on the configuration inside a conduit is the main target of this work. We, at first, anticipated the LTS conductor like SICC I has a large wetted perimeter and will be effective in heat removal. The temperature variations along the HTS stacks of various types of conductors can be found in Fig. 5. For SICC I, the heat loads are, in fact, stuck inside so that the temperature profiles looks quite similar to the stepwise heating profile presented in Fig. 4. For SICC I, we cannot charge the magnet up to 12 T. Quench occurred when the magnet charged to $\sim$8 T, at around 2400 seconds. On the other hand, for SICC II and III, dynamic temperature variations can be observed. The peak temperature is not located in the middle but moves toward the outlet as time goes on. For both SICC II and III, the magnet can be charged to 12 T, while the maximum temperature remains well below their current sharing temperature, 42.4 K.

The difference between SICC I and SICC III can be more clearly seen in Fig. 6, where the pressure, temperature and mass flow variations at the inlet and outlet are presented. The flow rate of SICC I is more than 10 times lower than that of SICC III. Another notable difference can be found in temperature variations. At first, the circulator is turned on, cryogen starts to flow, the inlet temperature is increased and the outlet temperature decreased due to Joule-Thompson effect, for both SICC I and

III. 50 seconds later, magnet charging starts. The temperature increase inside the conduit due to hysteresis loss also can be directly observed at the outlet of SICC III, whereas at the outlet of SICC I, temperature remains more or less the same, around 20 K. Furthermore, for SICC III, it can be observed that the cryogen temperature recovers its original value within 10 minutes as soon as the charging stops. If we can detect the temperature variation inside a conduit from the outlet temperature as immediately as discussed above and the heat load can be so quickly removed, then it may affect protection schemes as well. It was already reported that for a short HTS conductor, after heat above minimum quench energy is imposed, the temperature rise is not as fast as can be typically observed for LTS conductors, rather slow thermal runaway behavior can be observed [16].

The above results do not necessarily mean that SICC I is not appropriate for TF applications. Due to limited space, slow charging case results, 2.5 kA/hour, similar to CFS charging rate, are not presented here. But in this case, maximum temperature rise within SICC I conductor is $\sim$37 K and can be operated without quench. SICC I may be more effective in reducing temperature gradient within HTS stacks. As SUPERMAGNET code is a 1D model, temperature gradient which may occur inside the stacks of SICC II or III cannot be properly simulated. Also it should be noted coupling loss is not considered in this work. It is argued that coupling loss for non-twisted stacks behave like a monolithic superconductor. The coupling current has the same magnitude of the screening current [2]. Further empirical study on coupling loss for non-transposed stacks seems to be needed. Finally, there can be localized stress inside a conduit due to screening current. We may need additional support structure as schematically shown in Fig. 2(c) as 'alternative design'.

IV. CONCLUSION

In this work, non-transposed, cryogen-cooled 3 types of HTS conductors for fusion TF magnet applications are proposed; 1) LTS like porous type, 2) Segregated copper and HTS stack type

and finally 3) Only stacks without copper type. KSTAR size, 12 T max field thermo-hydraulic model was constructed and fast ramping case, 50 kA/hour, was studied. It was found type 2) and 3), SICC II and III, are very effective in removing the huge heat load generated by hysteresis loss. However, temperature gradient within stacks, impacts of coupling loss or screening current and so on need to be further studied. Further works including small size trial fabrications, are being conducted.

REFERENCES

[1] P. Bruzzone, "30 years of conductors for fusion: A summary and perspectives," *IEEE Trans. Appl. Supercond.*, vol. 16, no. 2, pp. 839–844, Jun. 2006.

[2] D. Ugliettia, R. Kang, R. Wesche, and F. Grillic, "Non-twisted stacks of coated conductors for magnets: Analysis of inductance and AC losses," *Cryogenics*, vol. 110, 2020, Art. no. 103118.

[3] L. Bottura, "Stability and protection of CICCs: An updated designer's view," *Cryogenics*, vol. 38, pp. 491–502, 1998.

[4] L. Bottura, "Cable stability," *Supercond. Accelerators*, pp. 783–789, 2013. [Online]. Available: https://indico.cern.ch/event/194284/contributions/1472820/attachments/281526/393608/StabilityScript.pdf

[5] Z. Hartwig, "The SPARC toroidal field model coil," in *Proc. 27th Int. Conf. Magnet Technol*. [Online]. Available: https://indico.cern.ch/event/975584/contributions/4430919/attachments/2352866/4014284/TFMC_FinalPresentation_MT27_Hartwig.pdf

[6] K. Kim et al., "Status of the KSTAR superconducting magnet system development," *Nucl. Fusion*, vol. 45, 2005, Art. no. 783.

[7] H. J. Ahn et al., "Engineering design status of the KSTAR TF coil structure," *IEEE Trans. Appl. Supercond.*, vol. 12, no. 1, pp. 492–495, Mar. 2002.

[8] J. Barber, J. Brisson, and J. Minervini, "Forced flow cooling of high field, REBCO-based, fusion magnets using supercritical hydrogen, helium, and neon," *Cryogenics*, vol. 96, pp. 34–43, 2018.

[9] Z. Hartwig et al., "VIPER: An industrially scalable high-current high-temperature superconductor cable," *Supercond. Sci. Technol.*, vol. 33, 2020, Art. no. 11LT01.

[10] N. Yanagi et al., "Design progress on the high-temperature superconducting coil option for the heliotron-type fusion energy reactor FFHR," *Fusion Sci. Technol.*, vol. 60, pp. 648–652, 2011.

[11] N. Yanagi et al., "Magnet design with 100-kA HTS STARS conductors for the helical fusion reactor," *Cryogenics*, vol. 80, 2016, Art. no. 243.

[12] S. Oh, H. W. Kim, Y. Chu, and D.-S. Park, "Dynamic simulation on flow characteristics of KSTAR PF magnet cryogenic network," *Fusion Eng. Des.*, vol. 174, 2022, Art. no. 112970.

[13] E. Pardo et al., "The transverse critical-state susceptibility of rectangular bars," *Supercond. Sci. Technol.*, vol. 17, 2004, Art. no. 537.

[14] M. N. Wilson, *Superconducting Magnets*. Oxford, U.K.: Oxford Univ. Press, 1983.

[15] R. Heller, P. Blanchier, W. H. Fietz, and M. J. Wolf, "Quench analysis of the HTS crossconductor for a toroidal field coil," *IEEE Trans. Appl. Supercond.*, vol. 29, no. 7, Oct. 2019, Art. 4703111.

[16] S. Hahn et al., "Design study on a 100-kA/20-K HTS cable for fusion magnets," *IEEE Trans. Appl. Supercond.*, vol. 25, no. 3, Jun. 2015, Art. no. 4801605.